Electron capture by slow multicharged ions in atomic and molecular hydrogen

D. H. Crandall, R. A. Phaneuf, and F. W. Meyer
Oak Ridge National Laboratory, Oak Ridge, Tennessee 37830
(Received 5 July 1978)

Measured cross sections for electron capture by a variety of multiply charged ions in collisions with atomic and molecular hydrogen are presented. The data are primarily for He-like and Li-like ions of B, C, N, and O in the velocity range $0.4–1.0 \times 10^8$ cm/sec. The electron-capture cross sections for these ions are typically 3×10^{-15} cm^2 in the velocity range tested. Comparison is made between these data and a number of recent theoretical predictions. While no simple scaling rules apply to these low-velocity data, for initial charge $q \geq +4$ the cross sections are essentially characterized by initial ionic charge rather than by projectile mass or electronic structure.

I. INTRODUCTION

Electron capture during collision of two atomic particles is an important basic process which has proven difficult to compute accurately. For multicharged ions ($q \geq 3$) in collisions at velocities below 2×10^8 cm/sec, the cross sections are large (up to 10^{-14} cm^2), so that this process is important in physical situations where such collisions occur. Recent theoretical research on electron capture with multicharged ions at low velocity has included both approximate or generalized estimates[1-7] and detailed calculations for specific collision partners.[8-13]

At low collision velocity the accepted theoretical models assume that the approaching atoms form a quasi-molecule, and the stationary states of this molecule (which can be represented in various ways) represent the colliding system at any given time or any internuclear separation. For collisions of a multicharged ion and a neutral atom resulting in electron capture, the initially separated atom and ion have an induced dipole attraction, while the finally separated two positive ions have a stronger, long-range Coulomb repulsion. Thus the difference in potential energy between the stationary states active in the electron-transfer process decreases during a collision process, and the probability of a collision-induced change from the initial state to a different final state is largest when the energy separation of the states is smallest. Within the well-known Landau-Zener approximation, electron transfer is considered to take place only at these "crossings" of the stationary states. More generally, the probability of transfer between stationary states is influenced by the coupling between the states, the collision velocity, and transitions at internuclear separations other than the one identified as the stationary-state crossing point.

For collisions of a highly charged ion and a many-electron atom, the number of state crossings which occur during a collision is large, a fact which can be generalized to give semiquantitative information about the electron-capture cross section.[1,3,4,6] For cases with many crossings, the total electron-capture cross sections are expected to be large and insensitive to collision velocity because of the number of crossings contributing to the total cross sections. The observations of Klinger, Müller, and Salzborn[14,15] for systems like Ar^{6+} + Ar agree with these generalized predictions.

For the collisions studied here with the atomic hydrogen target, there are only a few or no stationary-state crossings so that the cross-section behavior cannot be as generally predicted and specific cases must be investigated individually. Calculations which have been performed range from Landau-Zener with selected curve crossings[2] to coupled-state calculations including rotational coupling (of states with different symmetry) and transitions away from crossing points.[8-13] Except for some work on C^{4+} and B^{3+} collisions with atomic hydrogen[8] and helium[16-20] (where reasonable agreement is obtained with experiment within the experimental velocity range), the calculations have been for fully stripped ions incident on atomic hydrogen.[9-13] Since this collision system is a one-electron diatomic molecule, accurate stationary-state energies can be determined. However, calculations of electron capture for these systems are still approximate and give varying results depending on the states and types of transitions included.

The present paper presents measured cross sections for electron transfer between multicharged ions and atomic hydrogen which can test these calculations. We can present only one data point for a fully stripped incident ion (B^{5+}), but some of the other cases studied should also compare directly to the one-electron diatomic molecular

predictions. For collisions like $O^{6+} + H \rightarrow O^{5+} + H^+$, the tightly bound electrons on the incident ion are energetically well removed from the state of the captured electron. Thus, for the stationary states active in the electron-capture transitions, the presence of the electrons on the incident ion does not significantly perturb the potential energies from what they would be for $C^{6+} + H$ (the corresponding one-electron diatomic molecule). A similar argument for the case of $C^{4+} + H$ corresponding to $Be^{4+} + H$ has been made by Harel and Salin.[11] For high-velocity collisions, electron capture has been shown to be independent of the electrons remaining on the incident ion,[21-25] but that conclusion does not carry over directly to the low-velocity region where the molecular model applies.

For electron-capture studies atomic hydrogen is the most important target for testing theory, and in addition is the most relevant to applied problems. In astrophysics, charge exchange is an important mechanism which reduces the ionization state of multicharged ions, especially in the photon-ionized interstellar medium,[26-29] where the multicharged ions collide primarily with hydrogen and helium at very low velocity. Butler *et al.*[30] have pointed out that even in the absence of a significant state crossing contribution, electron capture can be important in astrophysics. In the high-temperature plasmas of fusion energy research, electron capture by multicharged ions from atomic hydrogen is dominant in determining penetration of injection-heating[31,32] and diagnostic[33] neutral beams. The role of electron capture by multicharged ions in atomic transport and spectral emissions in fusion energy plasmas has not been fully determined but is certainly important in specific cases. A particular example is the observation of Isler[34] on the ORMAK tokamak that electron transfer between injected atomic hydrogen and O^{8+} plasma impurity results in increased radiation from excited states of O^{7+}. Additional applied needs include understanding of light emissions in recombining plasmas[35,36] and use of electron transfer to excited states as a possible pump mechanism for short-wavelength lasers.[37,38]

Many of these applications require specific information on which excited states are populated by electron capture. This information is produced by the theories with multicharged ions incident on an atomic hydrogen target, but experimental test of excited-state populations is needed. Some experimental information on this question has recently been published,[39,40] but there are no data for an atomic hydrogen target.

II. EXPERIMENTAL TECHNIQUE

The present data were obtained by passing a beam of multicharged ions through a high-temperature oven of dissociated hydrogen (Fig. 1). When cold, the oven is a standard gas cell and is used to measure electron transfer in collisions with

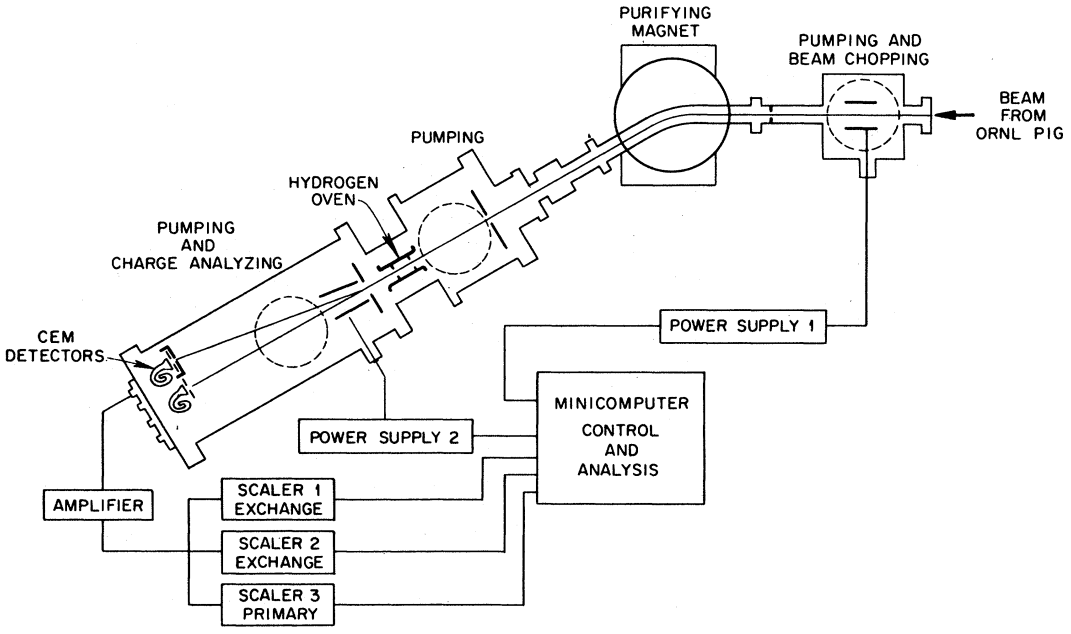

FIG. 1. Schematic of collision apparatus and experiment control.

molecular hydrogen, and when maintained at a typical temperature of 2350 K, it dissociates about 96% of the molecular hydrogen to separate atoms.

The ion source, the ORNL-PIG, has been described[41] and produces ion beams at energies from (4 kV)q to (25 kV)q, where q is the ion net charge, so that for ions used in the present study the velocities range from 0.4×10^8 to 1.2×10^8 cm/sec.

The ions from the ORNL-PIG were selected for given m/q by crossed electric and magnetic fields at the source and were additionally analyzed by the purifying magnet (Fig. 1) which removed ion charge states formed by charge-changing collisions in the transport of the beam from the source to the target. The geometry of the beams was determined by several apertures, the most restrictive being the 0.25-mm diam. entrance to the oven. Little angular divergence was present in the incident beam or was introduced by the scattering associated with electron transfer. This conclusion was demonstrated for the present case by scanning the charge-exchanged beam across the 5-mm diam. opening of the aperture in front of the off-axis channeltron (CEM) by varying the voltage on the analyzer deflector plates. The observed signal during such a scan was "flat-topped" with width greater than 5 times as large as the rise (and fall) width as the beam was cut off by the aperture, indicating a beam size for the charge-transferred component of less than 1 mm at the detector.

Control of the experiment and analysis of data were facilitated by an on-line minicomputer, as indicated schematically in Fig. 1. The incident ion beam was switched off manually or by the computer through power supply No. 1, which applied voltage to the deflector plates before the purifying magnet. After the ions were passed through the oven, about 2% of them had undergone electron transfer. For ion beam tuning the entire ion flux was detected by the on-axis CEM, while the electron-capture measurements used only the off-axis CEM. For cross-section measurements, the computer programmed the analyzer deflector (whose voltage was supplied by power supply No. 2) to deflect the desired charge-state component of the ion beam onto the off-axis CEM. During data collection, the computer gated the three scalers so that scaler 1 counted charge-exchange signal when the ion-beam component which had picked up one electron was selected by the deflector plates; scaler 2 counted only background from oven-produced photons and CEM dark when the same conditions were set as for scaler 1 except that the ion beam was completely shut off by the deflector before the purifying magnet; and scaler 3 counted the primary ions when the original ionic charge was selected by the analyzing deflector. The computer was programmed to alternately select each beam component and the background for a given time and to cycle through several repeats of the scheme to average over any beam fluctuations. The measurements were performed with gas in the oven and, separately, with an equal flow of gas "dumped" directly into the vacuum system—not through the oven—so that signal due to only the gas confined in the oven could be isolated (see Refs. 22 and 42). Linearity of the net charge-transfer signals with target gas flow was established for target thicknesses as high as 3 times those typically used for the measurements. The use of the computer allowed immediate data analysis and separation of signal from background for signals less than 1 count/sec. Cross sections were always measured for both H_2 and H targets (oven cold and oven hot), and the measured signal for H was corrected for the small residual amount of undissociated H_2 in the hot oven.

The operation and calibration of the hydrogen oven were the same as described in Ref. 22. The hydrogen dissociation fraction was measured using a 20-keV proton beam and observing the decrease in double-electron capture (H^- formation) as the oven was heated.[43] The effective target thicknesses (atom or molecule density times gas cell length) were determined by normalization to established cross sections, also using the 20-keV proton beam. For H_2, the value of 6.0×10^{-16} cm^2 was taken[44,45] as the correct single-electron-capture cross section for 20-keV protons, while for the H target, the value 5.2×10^{-16} cm^2 was used[45-47] for the normalization. Application of gas kinetic theory for the target geometry and gas flow employed gives target thickness estimates in excellent agreement with those obtained by the normalization procedure for both cold and hot oven conditions,[22] but the gas kinetic estimate is not considered to be as reliable for absolute target thickness determination as the normalization procedure used. Target thickness calibration and dissociation measurements were performed several months before and immediately after the present data were acquired, and the results were identical within the statistics of the individual measurements (see Table I).

III. UNCERTAINTIES

The estimated uncertainties in measured cross-section values are the same as those reported previously,[22] with two minor exceptions. Since the

TABLE I. Summary of systematic uncertainties in percent.

Source	$\sigma_{q,q-1}(H)$	$\sigma_{q,q-1}(H_2)$
Ion-beam purity (maximum effect on σ)	2	2
Beam collection and counting efficiency	5	5
Target gas purity (maximum effect on σ)	3	6
Determination of target thickness		
Reproducibility of calibration (90% CL)	5	3
Measurement of relative target cell gas flow	2	2
Reproducibility of oven temperature	2	2
Uncertainty in dissociation fraction	4	
Uncertainty in cross section used for normalization	10	10
Quadrature sum	13.5%	13.5%

ions are produced directly in the source, the crossed electric and magnetic fields provide complete isolation of a given ion charge and species, except for a few cases where ions have nearly identical m/q. For these cases (e.g., C^{3+} and O^{4+}, Ar^{5+}, and O^{2+}), the species purity depends on elimination of undesired gas in the ion source, but any remaining impurity in the beam can be analyzed by the apparatus used for the present studies (see Refs. 48 and 49) and correction for the impurity is made. The ions produced for the present study are expected to contain fewer metastable ions than beams produced by stripping in foils.[22] Studies of electron-impact ionization, which are currently in progress using the ORNL-PIG source, reveal the presence of metastables in the beam through ionization occurring at electron energies below that required for ionizing ground-state ions. At present such studies indicate the following typical fractions of metastables: (i) Li-like ion beams—B^{2+}, C^{3+}, N^{4+}, O^{5+}—have no metastables; (ii) B-like and Be-like ion beams—O^{3+}, N^{3+}—contain 10%–30% of the beam in metastable states with energies near the ground state; (iii) He-like ion beams—B^{3+}—contain about 1% metastables, while C^{4+} (and higher charges) definitely contain less than 1% and probably less than 10^{-3} fraction of metastables; and (iv) H-like ion beams—C^{5+} and B^{4+}—are estimated to contain less than 10^{-3} metastables because, as in the He-like cases, the energy to produce the metastables in the ion source plasma is near the energy to produce the next-higher ion state, which is greatly reduced in the ion source output. In general, the incident ion beam is well characterized, and the uncertainty in measured cross sections due to uncertainty in incident-ion beam purity (first line of Table I) is less for the present study than in the previous work.[22] However, a minor difficulty was encountered in counting the number of incident ions for the present study. Modulation of the ion beam at the source at rf frequencies (~100 kHz) occurred on some occasions. This modulation was detected as bunching of the incident ions in time at the modulation frequency and appeared to be a fluctuation of the ion source plasma. By careful specific control of ion source gas flow, the modulation could be reduced. Because of the time bunching of the beam, the instantaneous count rate for measurement of incident-ion flux could in some cases exceed the counting capabilities of the CEM detectors. This difficulty was not encountered in the previous measurements on H_2 target,[49] but an attempt to eliminate the problem through better regulation of the ion source arc supply was not completely successful. Thus it was necessary to monitor the temporal distribution of the incident-ion flux during data collection to assure that beam bunching was not occurring or to reduce the incident-ion flux sufficiently to ensure 100% counting efficiency. By measuring the apparent cross sections as functions of the incident-ion flux, we have established that the present data are free of significant error due to failure to adequately count incident ions, but we have allowed ±5% for absolute uncertainty in beam collection and counting (Table I) because of the difficulties encountered.

Table I lists the systematic uncertainties totaling to ±13.5% for both H_2 and H targets. The individual sources of systematic uncertainty were estimated at good confidence intended to be equivalent to 90% confidence level on statistics. The cross-section values used for normalization of target thickness values are estimated to be accurate to ±10%; this value is included in the 13.5% total systematic uncertainty. The total absolute uncertainty for each data point is obtained by combining this systematic uncertainty in quadrature with two standard deviations on counting

TABLE II. Electron-transfer cross sections $\sigma_{q,q-1}$ for multicharged ions capturing one electron from H and H_2.[a]

Ion	v (10^8 cm/sec)	$\sigma_{q,q-1}(H)$ (10^{-16} cm^2)	$\sigma_{q,q-1}(H_2)$ (10^{-16} cm^2)
B^{2+}	0.43	11.8(2.0)	20.4(0.8)
	0.47	14.2(1.2)	20.3(0.6)
	0.66	18.5(1.2)	17.8(0.4)
	0.73	15.8(1.4)	17.9(0.6)
	0.75	17.4(1.6)	18.4(0.8)
B^{3+}	0.52	3.3(0.6)	5.4(0.3)
	0.57	4.3(0.5)	6.4(0.2)
	0.73	9.3(0.7)	5.0(0.2)
	0.81	8.7(1.1)	8.3(0.3)
	0.92	10.6(0.8)	8.5(0.6)
C^{3+}	0.73	16.3(1.8)	6.4(0.3)
N^{3+}	0.51	20.8(1.2)	6.4(0.5)
	0.58	19.3(0.8)	6.8(0.4)
	0.72	17.7(0.8)	6.8(0.2)
	0.86	18.7(0.8)	7.9(0.3)
	0.99	15.8(1.2)	9.4(0.4)
B^{4+}	0.60	30.9(2.8)	22.1(1.0)
	0.66	26.5(1.6)	22.7(0.6)
	0.94	25.1(2.4)	23.0(0.8)
	1.06	27.2(1.0)	23.3(0.6)
C^{4+}	0.48	28.8(1.4)	26.6(0.6)
	0.58	27.5(2.0)	24.8(1.2)
	0.66	32.7(1.8)	25.9(0.8)
	0.73	29.3(2.6)	23.6(0.8)
	0.84	28.5(2.6)	23.2(1.2)
	0.99	28.2(2.6)	22.4(0.8)
	1.06	27.3(2.2)	21.7(1.0)
N^{4+}	0.44	29.2(1.0)	34.0(0.8)
	0.55	30.5(1.0)	33.8(0.6)
	0.59	26.0(4.8)	29.6(1.4)
	0.64	29.2(0.6)	30.8(0.4)
	0.73	29.5(1.0)	31.4(1.2)
	0.84	26.2(0.8)	27.0(0.4)
	0.99	24.4(0.8)	25.2(0.4)
	1.16	25.0(1.2)	28.1(1.2)
B^{5+}	1.05	22.6(4.0)	22.8(3.4)
C^{5+}	0.82	29.2(9.2)	20.0(1.4)
N^{5+}	0.51	20.3(2.8)	13.0(0.6)
	0.62	25.4(0.6)	18.3(0.3)
	0.67	24.6(1.4)	17.9(1.4)
	0.72	26.7(1.2)	19.7(0.6)
	0.82	27.2(1.4)	22.5(0.4)
	0.94	29.6(1.0)	21.7(0.8)
	1.11	33.1(2.2)	23.2(0.6)
	1.29	30.0(2.6)	26.3(1.0)
O^{5+}	0.56	27.8(3.6)	18.4(0.6)
	0.61	32.7(2.2)	22.0(1.4)
	0.73	34.8(2.0)	22.4(1.0)
	0.87	30.4(2.2)	22.1(0.8)
	0.98	32.4(1.0)	22.8(0.6)
O^{6+}	0.61	31.0(5.4)	35.9(2.8)
	0.67	37.7(6.8)	34.6(4.2)
	0.73	32.0(7.8)	33.9(1.8)
	0.95	37.6(3.8)	34.7(2.8)
	1.08	36.7(2.4)	34.3(1.4)
F^{6+}	0.73	35.5(2.2)	38.8(1.0)
Ar^{8+}	0.70	42.8(8.4)	34.9(1.6)

[a] Uncertainties in parentheses are 2 standard deviations on counting statistics and represent relative uncertainty. Total uncertainties are obtained by adding the tabulated statistical uncertainty in quadrature with systematic uncertainty of ±13.5% (Table I).

statistics (see Table II). A typical total uncertainty is ±16% at good confidence, dominated by the uncertainties in determining target thickness.

IV. RESULTS

A. General results

The measured cross sections for both H_2 and H targets for incident ions of B, C, N, O, and F are presented in Table II. Most of the data are for He-like and Li-like incident ions, but available data are presented for Be-like N^{3+}, H-like B^{4+} and C^{5+}, and fully stripped B^{5+}. For ions of charge 4+, 5+, or 6+ the forty measured values of electron transfer with atomic H have an average value of 29.2 (±3.8 s.d.) $\times 10^{-16}$ cm^2. As indicated by the small standard deviation, all these cross sections have approximately the same value. This feature is remarkable, indicating the lack of dependence of the electron transfer on the electronic structure of the incident ion, at least for incident ions with charge $q \geq 4$, where nearly all transfer is into excited states which are energetically well separated from the filled electronic states of the incident partially stripped ion.

The extent to which cross sections are grouped by incident-ion charge is illustrated in Fig. 2, which shows the measured cross sections for each charge q at 7.2×10^7 cm/sec for H_2 and H targets. While the cross sections are nearly the same for different species with a particular ionic charge, the cross sections do not scale according to any monotonic or simple rule as q changes. It has been noted previously for H_2 targets,[49] and for multielectron targets like Ar,[14] that at low velocity the σ_{54} cross sections are lower than σ_{43}, contrary to the simplest notion of scaling of σ with q. Also, σ_{32} seems to be anomalously low in the present data. The relatively small σ_{54} and σ_{32} cross sections can be attributed to the lack of a favorable molecular-state crossing for systems of these charges and will be discussed in more detail in individual comparisons.

B. Direct comparison with other experiments

1. Comparison with Gardner and Bayfield et al.

Two groups of experimenters have investigated collisions of multicharged ions with atomic hydrogen in the present energy range, using ions from the ORNL-PIG ion source. Figure 3 shows the preliminary results of Bayfield *et al.*[50] as renormalized by Gardner[51] and compares those values with values selected to be for the same ion species and velocity from present data and data of Phaneuf *et al.*[22] obtained with the present scattering apparatus. Although the magnitude of in-

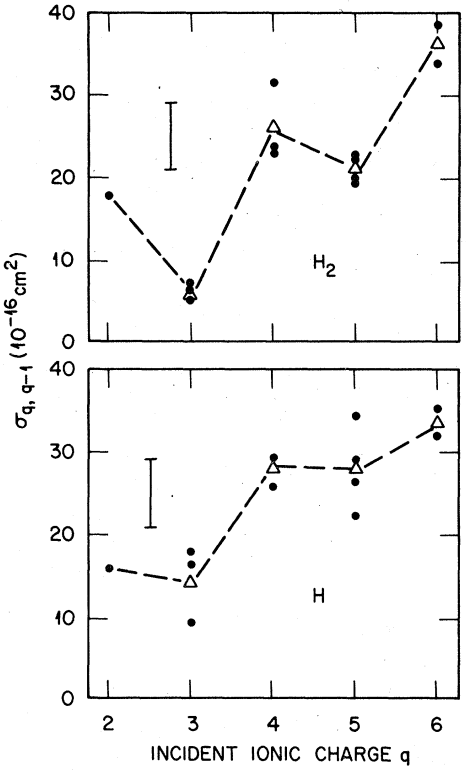

FIG. 2. Electron-capture cross sections as a function of initial ionic charge q for H and H_2 targets at collision velocity 0.73×10^8 cm/sec. Points are present data for various ions, and triangles are the average of the data value for a given q. Bars shown are typical total uncertainty for individual data points.

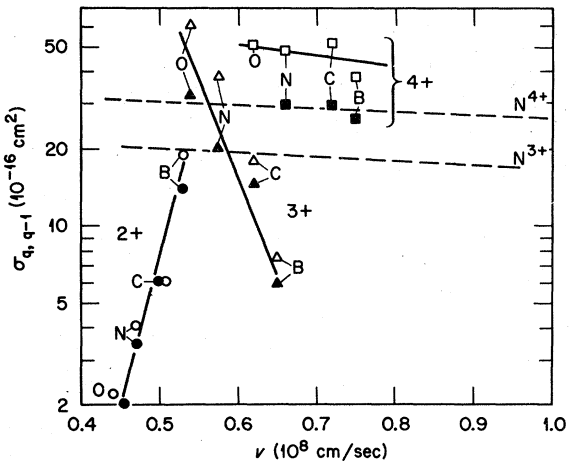

FIG. 3. Cross sections for electron capture by specific ions in atomic hydrogen (H). Open symbols are data of Bayfield *et al.* (Ref. 50) as corrected by Gardner (Ref. 51) for oxygen, carbon, nitrogen, and boron ions, with incident charge q indicated and various ions of given q connected by solid lines. Solid symbols are present data except that for 2+ ions data are extrapolated from values of Phaneuf, Meyer, and McKnight (Ref. 22) for the same ions. Circles, triangles, and squares represent data for ions of charge 2+, 3+, and 4+, respectively. Dashed lines represent present data for nitrogen ions of incident charge 3+ and 4+ as a function of collision velocity.

dividual cross sections is systematically lower for present data and for that of Ref. 22 compared to the values of Gardner and Bayfield *et al.*, the trends observed in the earlier data are substantiated.

The original data of Bayfield *et al.* were acquired by holding the extraction-acceleration potential fixed and obtaining as many different ions of charge 2^+, 3^+, and 4^+ as practical. As the mass and charge of the ion vary, the velocity of the collision varies slightly. As shown on Fig. 3 by the solid lines, for 2^+ and 3^+ ions the cross sections increased (2^+) and decreased (3^+) rapidly with reducing mass. This trend is now established not to be due to the small change in velocity of the ion, since data for N^{3+} at varying velocity have the trend shown by the dashed curve on Fig. 3. By contrast, for 4^+ ions (and for 5^+ or 6^+) change of the ion species (solid line) does not produce a different behavior from change in velocity for a given ion species (dashed line for N^{4+}). While we cannot claim any quantitative understanding of the steep and apparently linear variation of the 2^+ and 3^+ data with changing ion species, we believe the behavior is due to change in electronic configuration of the incident ion. For the 2^+ and 3^+ ions electron capture is dominantly into electronic shells (n levels) which already contain electrons so that the capture cross sections are influenced by the electronic structure of the incident ion. However, for ions of charge 4^+ or greater, electron capture is dominantly into higher electronic shells, $n=3$ or greater, which contain no electrons in any of the tested cases, so that the initial electronic structure of the ion has little influence on the cross sections, which no longer exhibit the strong species dependence. Thus we attribute the qualitative difference between the lower q (+2 and +3) capture cross sections and the higher q (+4 greater) cross sections to the generally held assertion that for higher q the capture is into more highly excited states.

The values given by Gardner[51] can be compared directly with present data for 17 individual data points for the atomic H target and 9 data points for the molecular H_2 target. For the H target the average ratio σ(Gardner)/σ(present data) is 1.54 ± 0.14 and for the H_2 target the average ratio is 0.86 ± 0.14, where the statistics on the ratios are 90% confidence level on the mean ratio for the number of cases compared.

The disagreement of the measured cross sec-

tions for atomic H is believed to derive from different techniques used to normalize the target thickness in the two sets of experiments. The oven used in the present experiments is heated directly by passage of current through the tungsten tube which is the wall of the gas containment cell.[45] This oven is very stable over time; that is, passage of a particular current through the tungsten tube produces a fixed, corresponding temperature even after hundreds of on-off cycles extended over more than two years of operation. Thus the dissociation fraction and target thickness could be determined using a 20-keV proton beam (as described) and a fixed oven-heating current. The results of such calibration before and immediately after the present data, as well as on several previous occasions, were identical within statistics (as discussed); it is inferred that the measured dissociation fraction, target thickness, and oven temperature were constant throughout all data measurements.

The oven used by Gardner and Bayfield *et al.* has desirable features (Ref. 52) derived from the fact that the gas containment cell is a thick-walled tungsten tube isolated inside a larger thin-walled tube used as a heater. Also, because the heater current is gated on and off, experiments can be done without possible effects of the associated magnetic field. However, these features require that instantaneous heater power be much higher than in the present oven, resulting in faster deterioration of the heater material and reduced stability of oven temperature versus applied power. The variation of temperature causes changes of target thickness which are accounted for by a different calibration technique. For their experiments the cross sections for Ar target gas are measured with the oven cold and with the oven heated in association with each measurement of a cross section for cold molecular and hot atomic hydrogen. The change of the charge-transfer signal for the Ar target with temperature is used as a thermometer to determine oven temperature (and as a check for any other spurious heating effects); the change of the capture signal level for the Ar target is taken directly to represent the temperature influence on target thickness for each individual measurement with hydrogen.

We believe the absolute value of the present results to be more reliable than those of Gardner and Bayfield *et al.*, but there is not absolute proof that this is the case. The technique using Ar as a thermometer relies on the temperature of the dissociated hydrogen being the same as that of Ar for a given cell wall temperature, which is not clearly established. A test using the Ar technique to calibrate our target thicknesses in the present data raised our results by about 20%—not enough to bring about agreement between the measurements, but more than our total estimated uncertainty. The data of Bayfield and Khayrallah[57] for $He^{2+}+H$, normalized using the Ar technique, are also higher by about 50% than data acquired with the present oven[53] and by other investigators.[54-56] The difference in the calibration technique seems to be the most likely source of the disagreement between present data and that of Gardner and Bayfield *et al.*[50,51] However, other differences in the experiments can be postulated as the source of disagreement, preventing absolute resolution as to which data are more reliable.

The reproducibility of the present data is better than that of Gardner,[51] who gives typical total uncertainty at ±30% with statistical quantities evaluated at 1 s.d. (67% confidence level), while the present data have a typical total uncertainty of ±16% with statistical uncertainties evaluated at 90% confidence level.

2. *Comparison with Crandall et al.*

The present molecular-hydrogen results can be compared directly to those of Crandall, Mallory, and Kocher.[49] Those earlier cross sections were obtained with completely different collision chamber and analysis system and are independently absolute. Absolute values were obtained in that experiment by direct measurement of pressure in the gas cell and measurement of effective gas cell length, while for the present data target thickness is obtained by normalization as described. For the molecular-hydrogen target the two experiments can be compared for 29 independent measurements of single-electron-capture cross sections. The average ratio, σ [Crandall *et al.* (H_2)]/σ[present (H_2)], is 1.016 (±0.019 at 90% confidence level on mean ratio), showing excellent agreement.

The previously published results of Phaneuf, Meyer, and McKnight[22] at higher velocities were acquired with the same collision apparatus but with a different source of ions. The only overlapping data are for N^{3+} near 60 keV where present data and those of Ref. 22 are identical for H and H_2 targets within counting statistics of either experiment alone.

C. Comparisons with theory

The most extensive direct comparison of present data and theory is for B^{3+} and C^{4+} incident on H which have been theoretically investigated by Olson, Shipsey, and Browne[8] (shown on Fig. 4). Their calculations employed configuration-interaction computation of molecular stationary-state

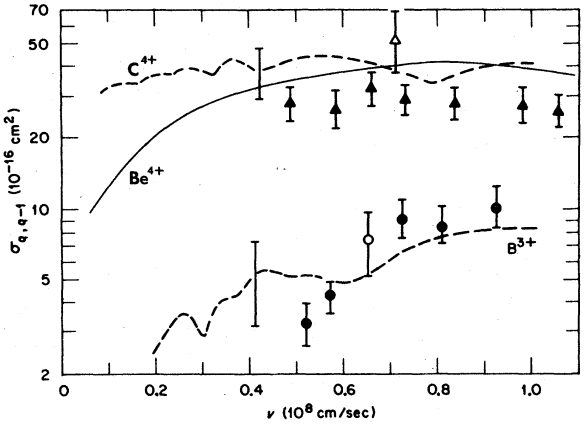

FIG. 4. Electron-capture cross sections for C^{4+} and B^{3+} in atomic hydrogen. Present data: ▲ for C^{4+} and ● for B^{3+}; data of Gardner and Bayfield *et al.* (Ref. 51): Δ for C^{4+} and O for B^{3+}. Dashed curves are theoretical results of Olson, Shipsey, and Browne (Ref. 8) for these ions, and solid curve is theoretical result of Harel and Salin for Be^{4+} (Ref. 11). Error bars on present data are total absolute uncertainties at good confidence intended to be equivalent to 90% confidence level on statistics.

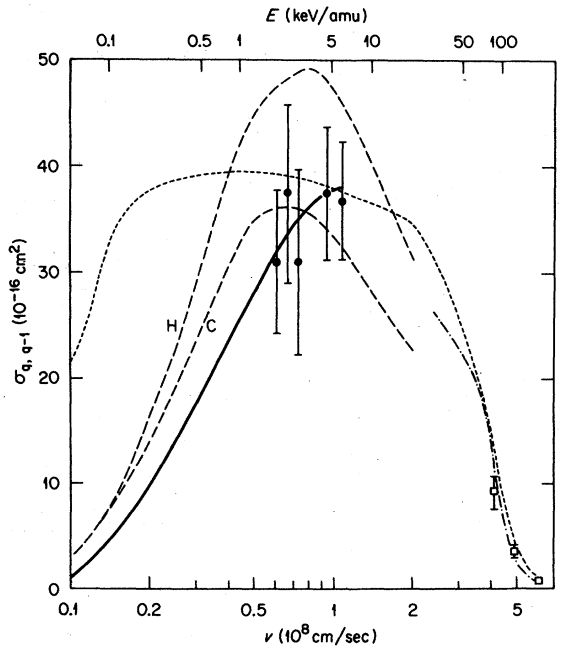

FIG. 5. Electron-capture cross sections for C^{6+} and O^{6+} in atomic hydrogen. Curves are theoretical results for C^{6+}: solid curve is from Vaaben and Briggs (Ref. 9), long-dashed curves are from Salop and Olson (Ref. 10) for coordinates centered on carbon (C) and for coordinates centered on hydrogen (H), short-dashed curve is from Ryufuku and Watanabe (Ref. 12), dash-dot curve is classical result of Olson and Salop (Refs. 10, 60). Data are for O^{6+} ions incident on H from present results (●) and from Meyer *et al.* (Ref. 61) (□).

potentials at nuclear separation of up to $10a_0$. They evaluated both radial and rotational coupling between the molecular states within a coordinate system centered on the center of mass of the colliding system without electron translational factors. Eight molecular states were included for $(BH)^{3+}$ and seven for $(CH)^{4+}$. The two cases are significantly different in that there are no molecular-state crossing points for $(BH)^{3+}$ and the resultant calculated cross section is relatively smaller (and estimated to be more uncertain) than for $(CH)^{4+}$, where distinct crossing points for states separating to $H^+ + C^{3+}$ $(1s^2, 3\ell)$ dominate the cross section. The error bars shown on the theory of Olson, Shipsey, and Browne (Fig. 4) are their estimate of uncertainty in the calculated cross sections for the two cases (25% for C^{4+} and 40% for B^{3+}).

The present data and the calculation agree within combined total uncertainties of experiment and theory, although good confidence experimental uncertainties overlap the actual calculated values only for 2 of the 12 data points. The two data points of Gardner and Bayfield *et al.*[50,51] agree reasonably well with the calculations and present data.

Harel and Salin[11] have calculated $Be^{4+} + H$ electron transfer and find the Be^{3+} $(n=3)$ final state to be dominant. Their three-state calculations with only Be^{3+} $(n=3)$ final products are shown on Fig. 4. They suggest, by examination of the molecular-potential curves, that electron transfer for $Be^{4+} + H$ and $C^{4+} + H$ should be the same and, to the extent that only $n=3$ levels are populated, this is born out by the agreement apparent in Fig. 4.

Theoretically, the most widely studied case of present interest is $C^{6+} + H \rightarrow C^{5+} + H^+$.[2,9,10,58,59] We have not been able to obtain fully stripped carbon at low velocity, but since the cross section is supposed to be dominated by transfer to C^{5+} $(n=4)$, the $(OH)^{6+}$ system at a given velocity should have nearly the same molecular potentials for the important states and the cross sections should be nearly the same (see Fig. 5). However, the various theories are not so discrepant that present data can clearly distinguish between them. Apparently, an important difference between the coupled-molecular-state theories is the choice of center of the coordinate system in evaluating the coupling between states. The most detailed eleven-state calculation by Vaaben and Briggs[9] employs a translation factor that shifts the coordinate system during the collision and obtains excellent agreement with present data. Salop and Olson[10] computed cross sections in a six-state calculation, using coordinate systems centered on either the

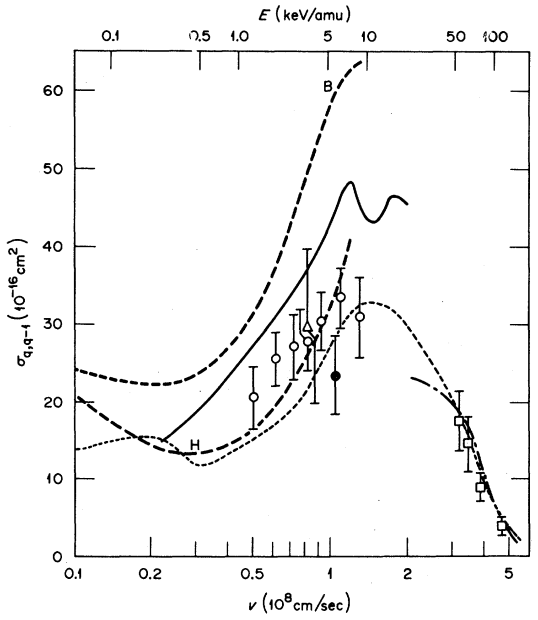

FIG. 6. Electron-capture cross section for 5+ ions in atomic hydrogen. Present data for B^{5+} (●), for N^{5+} (○) and for C^{5+} (△). Data of Phaneuf, Meyer, and McKnight (Ref. 22) for N^{5+} (□). Heavy dashed curve is a preliminary calculation of Salop and Olson for B^{5+} (Ref. 13) with coordinates centered on boron (B) and on hydrogen (H); solid curve is theory by Harel and Salin (Ref. 11) for B^{5+}; dot-dash curve is classical theory of Olson and Salop (Refs. 13 and 60); and short-dashed curve is UDWA theory by Ryufuku and Watanabe (Ref. 58).

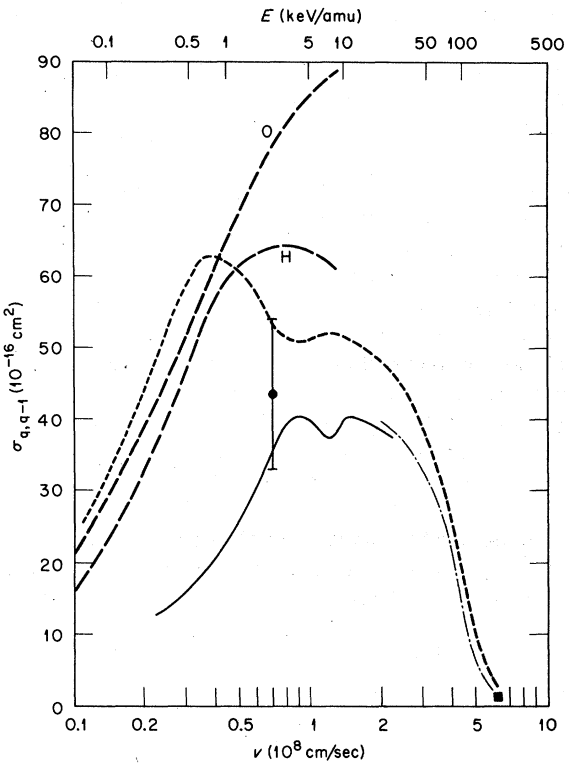

FIG. 7. Electron-capture cross sections for O^{8+} incident on atomic hydrogen. Curves are theoretical results: solid curve is from Harel and Salin (Ref. 11); long dashed curves are preliminary calculations of Salop and Olson (Ref. 13) for coordinates centered on oxygen (O) and on hydrogen (H); short-dashed curve is from Ryufuku and Watanabe (UDWA Ref. 12); and dot-dash curve is classical calculation of Olson and Salop (Refs. 13 and 60). Data are for O^{8+} from Meyer *et al.* (Ref. 61) (■), and present data for Ar^{8+} (●).

center of mass or the C or H nuclei. They chose to plot their results centered on H, which do not agree well with present data. However, their results centered on C and their two-state close-coupling results (not shown on Fig. 5) agree with present experiment and with Vaaben and Briggs in the energy range tested. Ryufuku and Watanabe[12,58] have carried through a detailed calculation within a different approach. They employ atomic orbitals in an "S-matrix" formulation to represent the system and calculate the charge-exchange amplitude employing unitarized distorted-wave approximation (UDWA) and other approximations. Their UDWA results extend over the complete velocity range and agree well with present data except for the lowest-energy data point. Experiments at lower velocities could provide a more sensitive test.

In the high-energy region the classical Monte Carlo calculation of Olson and Salop[10,13,60] and the UDWA of Ryufuku and Watanabe agree well with the recent results of Meyer *et al.*[61] for O^{6+}, with the low-energy theories tending smoothly toward the high-energy result.

The theoretical results for B^{5+} are more sensitive to the choice of coordinate center than similar results for C^{6+}, and perhaps B^{5+} is a more interesting case to test available theory. Our one data point for B^{5+} is lower than any of the theoretical estimates (Fig. 6). Invoking the same argument here as for the C^{6+} case, we compare the B^{5+} theory with present data for both C^{5+} and N^{5+}. These data are a little higher than the B^{5+} data and agree with the preliminary calculation of Salop and Olson[13] centered on H, at least over most of the tested velocity range. This agreement is opposite to the C^{6+} case, where agreement was with calculation centered on C; this reinforces the idea that the choice of coordinate system is not unique and that the inclusion of electron-translation factors may be necessary in some cases. The calculation of Harel and Salin[11] is again only a three-state calculation revealing the dominance of electron transfer of $B^{5+}+H$ resulting in B^{4+} ($n=4$); the values plotted in Fig. 6 are the sums of the transfers occurring from coupling of molecular states $5g\sigma - 4f\sigma$ and $5g\sigma - 3d\sigma$, with the first

transition dominating by about one order of magnitude. The Harel and Salin results are calculated with the origin of coordinate system fixed on the B^{5+} nucleus as in the upper curve of Salop and Olson (Fig. 6). The best agreement between B^{5+} data and theory is for the recent results of Ryufuku and Watanabe.[58]

For higher energies the classical Monte Carlo results of Olson and Salop[10,13,21,60] for 5+ ions agree well with data of Phaneuf, Meyer, and McKnight[22] for N^{5+} on H. However, unlike the C^{6+} case, for B^{5+} the low-velocity theories do not tend smoothly toward the high-energy results. For B^{5+} the various theories are discrepant at velocities near the Bohr orbit velocity ($v = 2.2 \times 10^8$ cm/sec), which suggests that this case is a sensitive one for testing theory in this difficult "transition" region of collision velocity.

Considerable theory has also recently appeared for $O^{8+}+H$ electron capture.[11-13] In this case the closest to a fully stripped projectile of charge 8 for which we have low-velocity data is Ar^{8+}. For the $(OH)^{8+}$ system, transfer is predicted to be dominantly into O^{7+} ($n = 5$) at low velocities, so that Ar^{8+} with outermost electrons in $n = 2$ levels may still be a fair representation of a fully stripped nucleus for electron transfer. Figure 7 presents the one data point we have obtained for $Ar^{8+}+H$. At high velocity the single experimental result of Meyer *et al.*[61] for O^{8+} projectile agrees well with the classical theory,[13,60] and the transition of theory from low-velocity to high-velocity regions is reasonably smooth, although not as good as for C^{6+}.

Additional general theoretical results and two-state results have been published which apply to the cases studied here (Refs. 2–7 and 59) but comparisons are not generally as favorable or as revealing as for the specific calculations represented in Figs. 4–7. Extension of studies with atomic H target to lower velocities than tested here and to excited-state formation through electron transfer would be fruitful for testing the developing theories and providing basic data of applied value.

ACKNOWLEDGMENTS

The authors are grateful to a number of people for supportive discussions throughout the experiments, most particularly to C. F. Barnett, R. E. Olson, J. S. Briggs, C. Bottcher, J. E. Bayfield, L. D. Gardner, and G. Lockwood. The design of the hydrogen oven was provided by G. W. McClure, and significant technical assistance was given by J. W. Hale and J. A. Ray. This research was sponsored by Divisions of Basic Energy Sciences and Magnetic Fusion Energy, U. S. Department of Energy, under Contract No. W-7405-eng-26 with the Union Carbide Corporation.

[1]R. E. Olson and A. Salop, Phys. Rev. A 14, 579 (1976).
[2]A. Salop and R. E. Olson, Phys. Rev. A 13, 1312 (1976).
[3]L. P. Presnyakov and A. D. Ulantsev, Kvant. Elektron. 1, 2377 (1974) [Sov. J. Quantum Elect. 4, 1320 (1975)].
[4]M. I. Chibisov, Pis'ma Zh. Eksp. Theor. Fiz. 24, 56 (1976) [JETP Lett. 24, 46 (1976)].
[5]A. Z. Msezane, Phys. Lett. A 59, 435 (1977); Phys. Rev. A 15, 2252 (1977).
[6]T. P. Grozdanov and R. K. Janev, Phys. Rev. A 17, 880 (1978).
[7]C. Bottcher, J. Phys. B 10, L213 (1977).
[8]R. E. Olson, E. J. Shipsey, and J. C. Browne, J. Phys. B 11, 699 (1978).
[9]J. Vaaben and J. S. Briggs, J. Phys. B 10, L521 (1977).
[10]A. Salop and R. E. Olson, Phys. Rev. A 16, 1811 (1977).
[11]C. Harel and A. Salin, J. Phys. B 10, 3511 (1977).
[12]H. Ryufuku and T. Watanabe, Phys. Rev. A (to be published).
[13]A. Salop and R. E. Olson (private communication).
[14]H. Klinger, A. Müller, and E. Salzborn, J. Phys. B 8, 230 (1975).
[15]A. Müller and E. Salzborn, Phys. Lett. A 62, 391 (1977).
[16]D. H. Crandall, R. E. Olson, E. J. Shipsey, and J. C. Browne, Phys. Rev. Lett. 36, 858 (1976).
[17]E. J. Shipsey, J. C. Browne, and R. E. Olson, Phys. Rev. A 15, 2166 (1977).
[18]D. H. Crandall, Phys. Rev. A 16, 958 (1977).
[19]H. J. Zwally and D. Koopman, Phys. Rev. A 2, 1851 (1970).
[20]H. J. Zwally and P. G. Cable, Phys. Rev. A 4, 2301 (1971).
[21]R. A. Phaneuf, F. W. Meyer, R. H. McKnight, R. E. Olson, and A. Salop, J. Phys. B 10, L425 (1977).
[22]R. A. Phaneuf, F. W. Meyer, and R. H. McKnight, Phys. Rev. A 17, 534 (1978).
[23]L. D. Gardner, J. E. Bayfield, P. M. Koch, H. J. Kim, and P. H. Stelson, Phys. Rev. A 16, 1415 (1977).
[24]H. J. Kim, P. Hvelplund, F. W. Meyer, R. A. Phaneuf, and P. H. Stelson, Phys. Rev. Lett. 40, 1635 (1978).
[25]R. E. Olson, K. H. Berkner, W. G. Graham, R. V. Pyle, A. S. Schlachter, and J. W. Stearns, Phys. Rev. Lett. 41, 163 (1978).
[26]A. Dalgarno and S. E. Butler, Comments At. Mol. Phys. 7, 129 (1978).
[27]R. A. McCray, C. Wright, and S. Hatchett, Astrophys. J. Lett. 211, L29 (1977).
[28]G. Steigman, Astrophys. J. 199, 642 (1975).
[29]R. B. Christensen, W. D. Watson, and R. J. Blint, Astrophys. J. 213, 712 (1977).
[30]S. E. Butler, S. L. Guberman, and A. Dalgarno, Phys. Rev. A 16, 500 (1977).
[31]J. T. Hogan and H. C. Howe, J. Nucl. Mater. 63, 151 (1976).
[32]D. H. Crandall, p. 157 in *Proceedings of the Fourth Conference on Scientific and Industrial Applications of Small Accelerators*, North Texas State Univ., edited by J. L. Duggan and J. A. Martin, available from IEEE

Service Center, 445 Hoes Lane, Piscataway, N. J. 08854.
[33]Equipe TFR, Nucl. Fusion 18, 647 (1978).
[34]R. C. Isler, Phys. Rev. Lett. 38, 1359 (1977).
[35]R. H. Dixon and R. C. Elton, Phys. Rev. Lett. 38, 1072 (1977).
[36]R. H. Dixon , J. F. Seely, and R. C. Elton, Phys. Rev. Lett. 40, 122 (1978).
[37]R. W. Waynant and R. C. Elton, Proc. IEEE 64, 1059 (1976).
[38]A. V. Vinogradov and I. I. Sobel'man, Zh. Eksp. Theor. Fiz. 63, 2113 (1976); [Sov. Phys. JETP 36, 1115 (1973)].
[39]V. V. Afrosimov, A. A. Basalaev, M. N. Panov, and G. A. Leiko, Pis'ma Zh. Eksp. Theor. Fiz. 26, 699 (1977) also p. 528 in *Abstracts of the Tenth International Conference on Physics of Electronic and Atomic Collisions*, edited by G. Watel (North-Holland, Amsterdam, 1976).
[40]H. Winter, E. Bloemen, and F. J. de Heer, J. Phys. B 10, L453 (1977).
[41]M. L. Mallory and D. H. Crandall, IEEE Trans. Nucl. Sci. 23, 1069 (1976).
[42]J. E. Bayfield, Phys. Rev. 182, 115 (1969).
[43]G. J. Lockwood, H. F. Helbig, and E. Everhart, J. Chem. Phys. 41, 3820 (1964).
[44]P. M. Stier and C. F. Barnett, Phys. Rev. 103, 896 (1956).
[45]G. W. McClure, Phys. Rev. 148, 47 (1966).
[46]J. E. Bayfield, Phys. Rev. 185, 105 (1969).
[47]I. M. Cheshire, D. F. Gallaher, and A. Joanna Taylor, J. Phys. B 3, 813 (1970).
[48]D. H. Crandall, P. O. Taylor, R. A. Phaneuf, Phys. Rev. A 18, 1911 (1970).
[49]D. H. Crandall, M. L. Mallory, and D. C. Kocher, Phys. Rev. A 15, 61 (1977).
[50]J. E. Bayfield, P. M. Koch, L. D. Gardner, I. A. Sellin, D. J. Pegg, R. S. Peterson, and D. H. Crandall, p. 126, in *Abstracts of the Fifth International Conference on Atomic Physics, Berkeley, 1976,* edited by R. Marrus, M. H. Prior, and H. A. Shugart (University of California, Berkeley, 1976)
[51]L. D. Gardner, thesis (Yale University, 1978) (unpublished).
[52]J. E. Bayfield, Rev. Sci. Instrum. 40, 869 (1969).
[53]R. E. Olson, A. Salop, R. A. Phaneuf, and F. W. Meyer, Phys. Rev. A 16, 1867 (1977).
[54]G. J. Lockwood, G. H. Miller, and J. M. Hoffman, Bull. Am. Phys. Soc. 21, 1266 (1976); also G. J. Lockwood (private communication). These data do not depend on any normalization procedure.
[55]W. L. Fite, A. C. H. Smith, R. F. Stebbings, Proc. R. Soc. Lond. A 268, 527 (1962).
[56]M. B. Shah and H. B. Gilbody, J. Phys. B 7, 630 (1974).
[57]J. A. Bayfield and G. A. Khayrallah, Phys. Rev. A 12, 869 (1975).
[58]H. Ryufuku and T. Watanabe (private communication).
[59]P. T. Greenland, J.Phys. B 11, L191 (1978).
[60]R. E. Olson and A. Salop, Phys. Rev. A 16, 531 (1977).
[61]F. W. Meyer, R. A. Phaneuf, H. J. Kim, P. Hvelplund, and P. H. Stelson, Phys. Rev. A (to be published).